Dear Editor and Reviewer:

Thank you very much for your insightful comments concerning our manuscript "High-resolution modeling the distribution of surface air pollutants and their intercontinental transport by a global tropospheric atmospheric chemistry source-receptor model (GNAQPMS-SM)" (MS No.: gmd-2021-201). Those comments are all very valuable and helpful for revising and improving our manuscript. We have studied comments carefully and have made revision. The point by point responses are as following:

Responds to the referee's comments:

Referee #1

Comment 1: line 67-69, 82, 85: The models name of "STEM", "CAMx", "MOZART-4", "GEOS-Chem", "CHASER", "TM5" (ant other models if used) are needed to be explained.

Response: Thank you for your comments. We have used the full name in the latest manuscript. STEM means sulfur transport and deposition model; CAMx means the Comprehensive Air Quality Model with Extensions; MOZART-4 means Model for Ozone and Related chemical Tracers, version 4; GEOS-Chem means the Goddard Earth Observing System model coupled to chemistry; CHASER means chemical atmospheric general circulation model for study of atmospheric environment and radiative forcing; TM5 is a Tracer Model version 5.

Comment 2: line 89-90: This sentence should be revised to define "GNAQPMS" first.

Response: Thank you for pointing out our improper description order. We have updated the corresponding statements in the latest manuscript at line 92-94 as the blue text below:

"In this study, by coupling an online S-R relationship module into the Global Nested Air Quality Prediction Modeling System (GNAQPMS), we developed a global tropospheric atmospheric chemistry source-receptor model (GNAQPMS-SM) and then conducted a 1-year high-resolution (0.5°×0.5°) simulation for 2018."

Comment 3: line 141: "each pollutant" (CT in this context) is "each tagged pollutant"?

Response: Thank you so much for your professional attitude and helping us correct an imprecise express. We have changed the expression from "each pollutant" to "each tagged pollutant".

Comment 4: line 145: After Eq. (1), the wording of "labeled" is used. Is this same to "tagged"? If this is different, the meaning of "label" should be explained. If this is same, it is better to unify the expression to avoid the confusion.

Response: Thank you for your suggestions. The word of "labeled" is same to "tagged", and we have unified the expression in the latest manuscript.

Comment 5: line 184: It seems to be better to define all abbreviations used in Fig. 1a here, or please prepare the table information (possibly within Table 1). It is confusing to be defined it every time used in discussion section.

Response: Thank you for your comments. We have added a table that defines all region abbreviations used in our manuscript in the supplement as the table below:

Table S1. The definition of tagged source regions used.

Source region	Definition
China	China
RBU	Russia, Belarussia, Ukraine
MCA	Mexico, Central America, Caribbean, Guyanas, Venezuela, Colombia
MDE	Middle East
SAF	Sub-Saharan/sub-Sahel Africa
NAF	Northern Africa, Sahara, Sahel
PAN	Pacific, Australia, New Zealand
SEA	South East Asia
SAS	South Asia
EUR	Europe
CAS	Central Asia, Mongolia
NAM	US + Canada
SAM	South America
SPO	Antarctic
South Korea	South Korea
Japan	Japan
North Korea	North Korea
NPO	the ocean north of 66.5° N
OCN	Non-arctic Ocean

Comment 6: line 198: Why NH$_3$ and NMVOC were prepared from different emission inventory? The description of these emissions has been provided; however, there is no reason to conform them. It should be stated. In addition, these emission years are also different from the simulation year (2018). I understood that the time-lag in emission inventories, but do the authors have reasonable reason (e.g, negligible change between 2015 and 2018) to use different emission in this simulation?

Response: Thank you for your constructive comments. Non-methane volatile organic compounds (NMVOC) include a large number of chemical species differing for their chemical composition and properties. EDGAR v5.0 only provides the total emissions of NMVOC, while EDGAR v4.3.2

disaggregates total NMVOC emissions into species which is better to simulate O_3 and secondary organic aerosols formation. Meanwhile, the global NMVOC emissions in 2015 published by EDGAR v5.0 are 150.5 Tg and the emissions in 2012 are 144.3 Tg. The 3-year change rate is 4.3%, with little change. Therefore, we chose EDGAR v4.3.2 emission inventory for NMVOC.

As shown in Fig. 1, comparing time series of EDAGR NH_3 emissions in China with those NH_3 emissions from Kong et al. (2019), Liu et al. (2019) and HTAP v2.2 (Janssens-Maenhout et al., 2015), EDGAR NH_3 emissions in China reach a maximum in spring and autumn, while other emission inventories peak in summer. Many studies have already proven that NH_3 volatilization rates are strongly modulated by environmental factors such as temperature and wind speed, which will strengthen in JJA in China due to the higher temperature (Kong et al., 2019; Zhou et al., 2016). Therefore, for NH_3, we used the HTAP v2.2 emission inventory instead of EDGAR v5.0. It's unclear stated in the manuscript and we have revised it in the latest manuscript at line 205-207 as the blue text below:

"NH_3 is adopted from the HTAP v2.2 emissions inventory for 2010 (Janssens-Maenhout et al., 2015; data available at https://edgar.jrc.ec.europa.eu/htap_v2/index.php?SECURE=123) because the NH_3 emissions in China from HTAP v2.2 inventory are more consistent with that from China regional inventories compared with EDGAR v5.0."
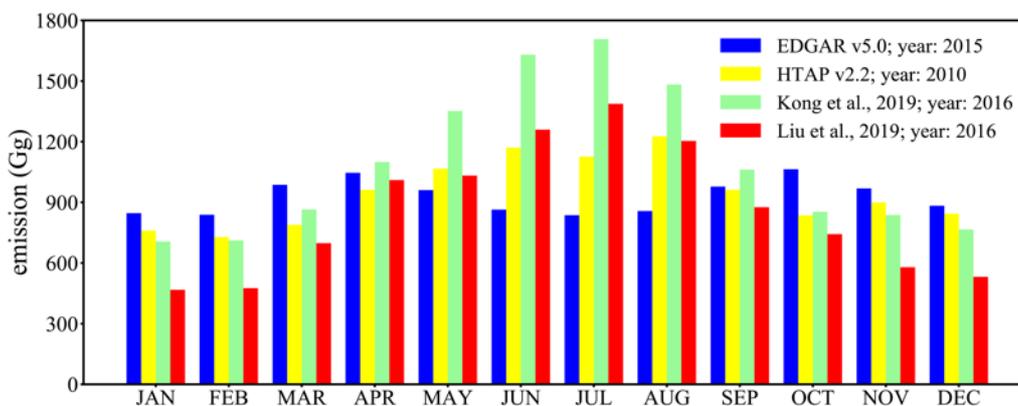
Figure 1. Time series of NH_3 emission in China from January to December in different emission inventories.

Thank you for understanding the time-lag in emission inventories. The official inventories made by countries or regions have at least a 1-year time lag (Janssens-Maenhout et al., 2015), and the global emission inventories, e.g., EDGAR has a nearly 5-year time lag and is currently updated to year 2015. In order to understand the possible influence on inconsistent inventory years on the results, we compared the 1-year change rate of pollutants emissions in three regions (NAM, EUR, China) as shown in Fig. 2. The 1-year change rate of BC in NAM ranges around $\pm10\%$ and in EUR ranges within $\pm5\%$. BC emissions in China have changed within $\pm10\%$ since 2010. The 1-year change rate of primary $PM_{2.5}$ in three regions are all within $\pm10\%$. The 1-year change rate of NO_x and SO_2 in three regions ranges within $\pm5\%$ and $\pm10\%$ since 2010, respectively. All change rates

are within the region and pollutant emission uncertainties (95% confidence interval) reported by Crippa et al. (2019). For example, the SO_2 emission uncertainty in China, USA, Canada is 12%, 31%, 53%, respectively. NAM refers to USA and Canada. Moreover, from the perspective of the 3-year change rate, global total emissions changed a little within ±5% between 2015 and 2012. We also computed the annual BC, SO_2, CO emissions in year 2017, 2018, 2019 from the Community Emissions Data System (CEDS) for Historical Emissions, their 1-year change rate of BC, SO_2 and CO ranges from -1.6% to -0.6%. It can be seen that there is no significant change of emission inventories between 2015 and 2018, and we have more observation data in China in 2018. Therefore, we chose the emission inventory 2015 to simulate the year 2018.

BC, NO_x, primary $PM_{2.5}$, SO_2 emissions in China have all decreased since 2014 due to the implementation of the toughest-ever clean air policy in China, and the decrease of SO_2 emissions is significant. Zhang et al. (2019) reported that from 2015 to 2017 SO_2 emissions in China decreased by 35%, while NO_x and NMVOC emissions changed slightly with a decrease lower than 10%. However, this significant SO_2 change is not reflected in our emission inventory, which should be a possible reason for the overestimation of SO_2 in China and may have an impact on our analysis of nss-sulphate transport from China to the downwind regions. We have added discussion about this part in the latest manuscript.
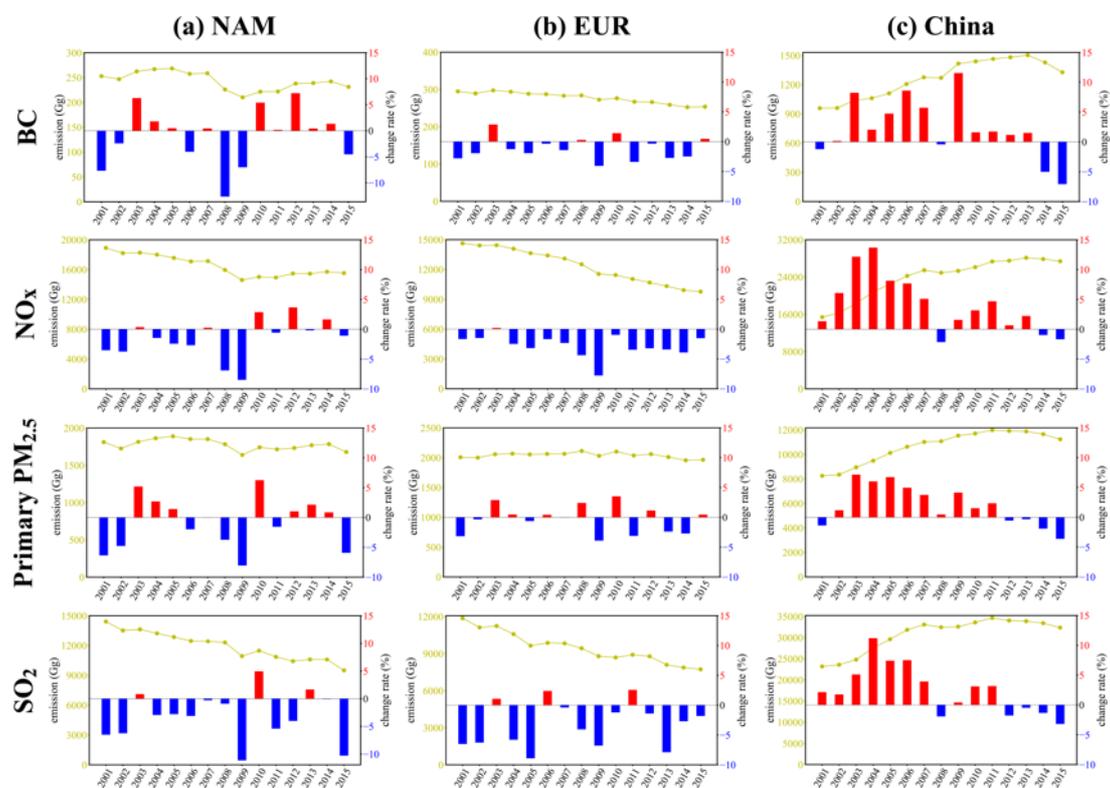
Figure. 2 Annual emissions and 1-year change rate of BC, NO_x, primary $PM_{2.5}$ and SO_2 in (a) NAM, (b) EUR, and (c) China from 2001 to 2015.

Comment 7: line 241-242: The information for MODIS is not sufficient. Which satellite, products and its resolution? In addition, the appropriate reference should be stated.

Response: Thank you for your comments. The level-3 atmosphere monthly global product (MOD08_M3) is used to evaluate the simulated AOD and it consists of approximately 800 statistically derived data sets (Platnick, 2015). The product contains monthly 1°×1° gird average values of atmospheric parameters. We have updated the corresponding statements at line 253-256 as the blue text below:

"The aerosol optical depth (AOD) from the level-3 atmosphere monthly global product (MOD08_M3; Platnick (2015); data available at https://ladsweb.modaps.eosdis.nasa.gov/archive/allData/-61/MOD08_M3/), retrieved from MODIS Terra, is used to evaluate the simulated AOD and the horizontal resolution is 1°×1°."

Comment 8: line 269: What stands for "BCC"?

Response: Thank you for your comments. BCC-GEOS-Chem is an online global atmospheric model, by coupling the GEOS-Chem chemical transport model as an atmospheric chemistry component in the Beijing Climate Center atmospheric general circulation model developed by Lu et al. (2020). We compared our model performance with BCC-GEOS-Chem model performance. We have revised it in the latest manuscript at line 286-288 as the blue text below:

"The model performance is similar to the BCC-GEOS-Chem (an online global atmospheric model, by coupling the GEOS-Chem chemical transport model as an atmospheric chemistry component in the Beijing Climate Center atmospheric general circulation model) performance reported by Lu et al. (2020)."

Comment 9: line 274-275: When did we find this injection? JJA? Figure 3 only represents annual averaged data and where can we trace the seasonality?

Response: Thank you for your constructive comments. As shown in Fig. 2a in the manuscript, O_3 mixing ratios in the Southern Hemisphere peaks in JJA, and we attribute this high value to the injection of stratospheric O_3. Figure 3 below compares the simulated seasonal mean O_3 vertical profiles with ozonesonde observations over the Southern Hemisphere. GNAQPMS captures the seasonality of O_3 concentration under 800 hPa, and O_3 reaches a maximum in JJA and a minimum in DJF. Above 200 hPa, O_3 concentration peaks in JJA, which is consistent with observations. We have added this figure to support our analysis in the latest supplement, and revised this sentence in the latest manuscript at line 294 as the blue text below:

", which is consistent with observations as shown in Fig. S2."
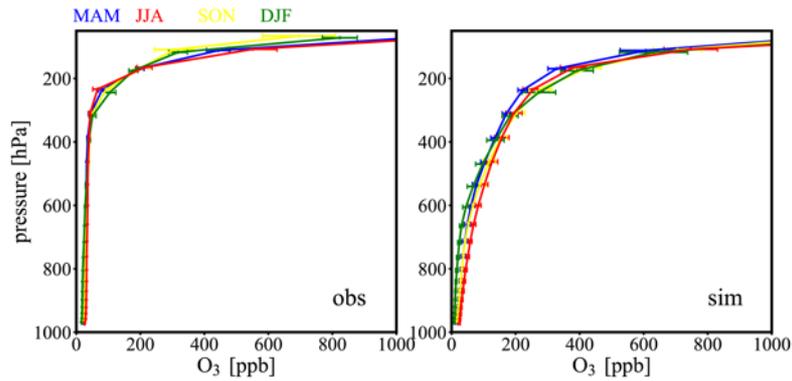
Figure 3. Comparisons of GNAQPMS-simulated seasonal mean ozone vertical profiles with ozonesonde observations averaged over the Southern Hemisphere.

Comment 10: line 308: What is the target year of these studies for CO? Remind that the simulation in this study is not consistent to the year of emission inventory.

Response: Thank you for your comments. The CO emissions used in Horowitz et al. (2020) is for year 2014, and in Myriokefalitakis et al. (2020) is for the year 2006. Figure 4 shows the change rate of annual total global CO emissions based on Edgar database. We assumed that the 1-year change rate of CO emissions of each inventory is the same. As shown in Fig. 4, the 1-year change rate of total global CO emissions ranges within ±5% from 2001 to 2015. The anthropogenic emission of CO in our study is higher than Horowitz et al. (2020) CO emissions, with increased rate 12%. Considering the large time difference between the target year 2006 we referred and year 2015 of our emission inventory, we have deleted the Myriokefalitakis et al. (2020) reference in the latest manuscript and have added the target year of the study at line 325 as the blue text below:

"The anthropogenic emission of CO in this study is 686.7 Tg/yr, which is higher than values in other studies, e.g., Horowitz et al. (2020) used 612.4 Tg/yr for year 2014."
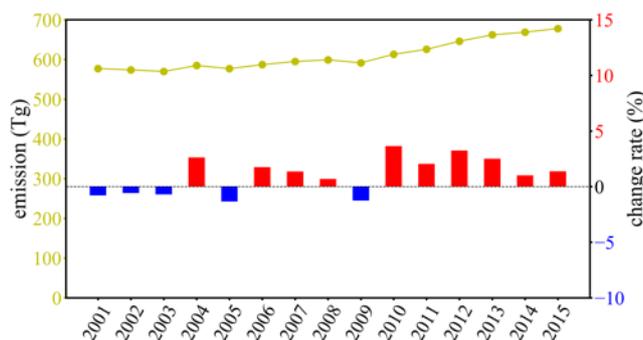
Figure 4. Annual total global emissions and annual change rate of CO according to EDGAR.

Comment 11: line 314 and Figure 4: I guess that white color indicated the deficit of measurement. The simulation result did not show such deficit, so are there no treatment to consider the measured

deficit grid in the model comparison? There is no available information of AK in TROPOMI retrieval? The comparison methodology was not provided enough.

Response: Thank you for your comments. The white color in Fig. 4b indicates missing measurement. The Tropospheric Monitoring Instrument (TROPOMI) was loaded onboard the Sentinel-5 satellite for fine gas monitoring (van Geffen et al., 2020). TROPOMI has a significant advantage over the previous sensor in spatial resolution and number of clear-sky observations per day (Guanter et al., 2015). The monthly tropospheric NO_2 column concentration data from the Royal Netherlands Meteorological Research Institute (KNMI) used in our paper has measurement loss in some areas. We compared the NO_2 columns through one-by-one correspondence between the simulation time and the TROPOMI data observed time, the model grid cell and TROPOMI data grid cell. The simulation results when drawing, are filled with model results if the grid cell misses measurement in the TROPOMI data. The horizontal resolution of our simulation is 0.5°×0.5° and the resolution of TROPOMI data is 0.125°×0.125°. In order to be consistent, in the latest manuscript we have eliminated the grid cells in our simulation which is missing in the TROPOMI data as shown in Fig. 5 below.
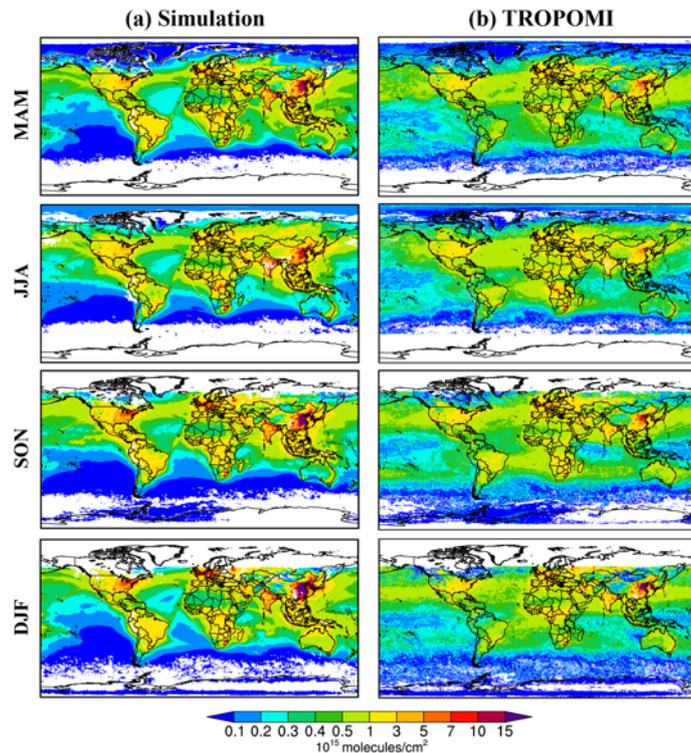
Figure 5. Spatial distributions of seasonal mean NO_2 columns from (a) GNAQPMS averaged in 2018 and (b) the TROPOMI data.

We have revised this part in the latest manuscript at line 250-258 as the blue text below:

"NO_2 columns are compared with tropospheric NO_2 column concentration data from the Tropospheric Monitoring Instrument (TROPOMI; van Geffen et al. (2020); data available at

http://www.temis.nl/airpollution/no2.php), and the resolution of monthly TROPOMI NO_2 data from the Royal Netherlands Meteorological Research Institute (KNMI) used in our paper is 0.125°×0.125°. … We compared the spatial distribution of AOD and NO_2 columns through one-by-one correspondence between the simulation time and the MODIS, TROPOMI observed time, the model grid cell and MODIS, TROPOMI data grid cell."

Comment 12: line 326 and Figure 5: Same comment on Figure 4, but in this case, model simulation was not shown over high-latitude region. Again, in addition to the lack of description on MODIS dataset, the comparison methodology was not given appropriately.

Response: Thank you for your comments. The level-3 atmosphere monthly global product (MOD08_M3) is used to evaluate the simulated AOD. The horizontal resolution of product is 1°×1° and the horizontal resolution of our simulation is 0.5°×0.5°. In Fig. 5a, the MODIS missing measurement mainly focuses on the north of 66.5 °N and the south of 66.5 °S. Therefore, we only showed the simulated AOD between 66.5 °S and 66.5 °N. We have revised this figure in the latest manuscript as Fig. 6 below. If there are deficit in the MODIS data grid cell, model simulation results were also not shown. Same reply on Comment 11, we compared the spatial distribution of AOD through one-by-one correspondence between the simulation time and the MODIS data observed time, the model grid cell and MODIS data grid cell.
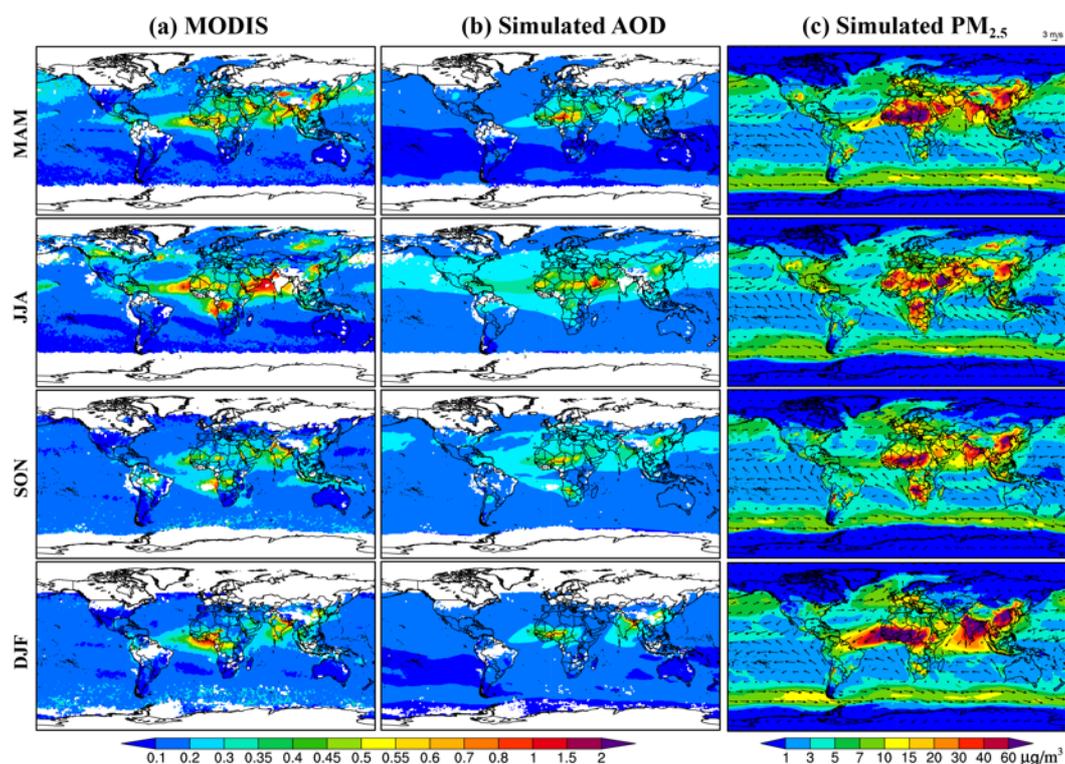
Figure 6. Spatial distributions of seasonal mean AOD at 550 nm from (a) MODIS data and (b) GNAQPMS averaged in 2018 and (c) PM$_{2.5}$ in GNAQPMS.

Comment 13: line 373-375: It is ambiguous that whether this is the additional experiment or included as presented study. If modeling results have been presented by including this emission inventory, this statement have to be explained in Section 2.4.

Response: Thank you for pointing out a negligence in the description of the emission inventory. We didn't carry out an additional experiment to verify the results in the cited references, but we added this emission inventory in our simulation. We have updated the corresponding statements in Section 2.4 at line 214-215 as the blue text below:

"FINN provides daily global emissions with a resolution of 0.1°×0.1° in 2018 based on satellite observations for detecting active fires as thermal anomalies and land cover change (Wiedinmyer et al., 2011). Gas flaring emissions ECLIPSE V5a (Klimont et al., 2017; https://iiasa.ac.at/web/home/research/researchPrograms/air/ECLIPSEv5a.html) are added in the inventory, and this will be mentioned later."

Comment 14: line 453: What means "large-scale"?

Response: Thank you for your comments. Large-scale refers to a larger domain, e.g., a domain covers the hemisphere or the world. We have revised the expression in the latest manuscript at line 473 as the blue text below:

", which also always appears in other regional or corresponding large-domain CMAQ or GEOS-Chem simulations"

Comment 15: line 472-473: Here mentioned on dust and sea-salt, but the analysis is focused on $PM_{2.5}$. I guess that PM_{10} could be largely affected by these natural sources whereas $PM_{2.5}$ would be mainly composed by anthropogenic sources. I can partly understand the following discussion, but for example, approximately half of $PM_{2.5}$ source over NAM is attributed to natural sources. Are these consistent to or different from other researches? Moreover, the configuration of source-receptor analysis posed "OCN". Did "OCN" source represent sea-salt sources? Why it was separated as natural sources?

Response: Thank you for your valuable comments. The analysis of our S-R relationship is based on the average of all grid cells in the receptor region. Except North and South Africa, Central Asia and western China, North America is also a potential dust source region (Tanaka and Chiba, 2006), e.g., Great Basin Desert, Chihuahuan Desert, Sonoran Desert, and Mojave Desert. They are all located in the western portion of the country. More than 30 percent of North America is comprised of arid or semi-arid lands, with about 40 percent of the continental United States at risk for desertification. It could lead to the uncertainty of our results. We select 3 stations around the deserts,

Joshua (33.75° N, 115.82° W), Preston (42.08° N, 111.86° W), Rangely (40.09° N, 108.76° W). Figure 7 shows the time series of dust contributions to surface $PM_{2.5}$ concentrations in the 3 stations. Dust aerosols contribute around 20% to 80% in Joshua in different months. The monthly average contributions of dust in Preston and Rangely change more than that in Joshua, only around 5% at low level and more than 90% at high level. They all reach the maximum in MAM and JJA. The annual contributions of dust in Joshua, Preston, Rangely are 59.8%, 45.9%, 62.5%, respectively. Andreae (1995) has pointed that more than 50% of the global atmosphere aerosols come from dust aerosols in deserts and their surrounding areas. Hand et al. (2017) pointed that fine mineral dust is a major component of $PM_{2.5}$ mass ($\geq$50%) during MAM at Southwest U.S., and DJF and SON contributions in the Southwest is lower but reach 35-40% at several sites in Nevada and California and along the U.S.-Mexico border for year 2011-2014, which is consistent with our near California Joshua station simulations. Here we simply attribute dust to the contribution of natural emissions, plus the contribution of other natural sources and sea salt, which leads to a heavy proportion of natural sources in our results.
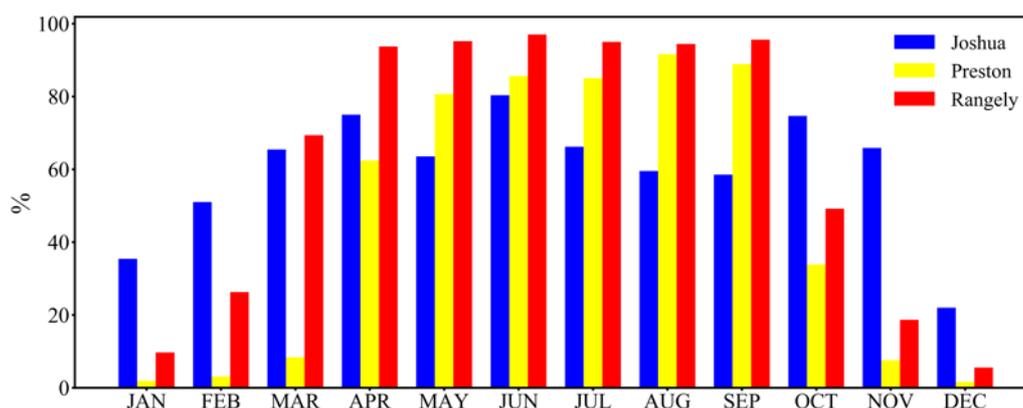
Figure 7. Dust contributions to surface $PM_{2.5}$ concentrations in 3 stations.

"OCN" source mainly represents transportation source category in OCN, that is, traffic source category. Traffic emissions e.g., aircraft and ship, can lead to the generation of pollutants on the source region OCN, then make contributions to the surrounding regions. Traffic emissions perturb the atmospheric composition mainly by the emission of NO_x, which by photochemical conversions causes an increase in O_3. Therefore, the source region OCN makes greater contributions to the surrounding receptor region on surface O_3 than that on surface $PM_{2.5}$, as shown in Fig. 13 and Fig. 14 in the manuscript. Near the coast of continents, there exists O_3 transportation with substantial contributions from source region OCN. Meijer et al. (2000) already pointed that aircraft contributes about 10% to the O_3 concentration in the North Atlantic flight corridor and surface emissions contributes about 20% and 30% to the O_3 concentration of surface ocean. Therefore, it's separated from natural sources. We have revised the sentence in the latest manuscript at line 554-555 as the blue text below:

"Nearly 25% of global anthropogenic NO$_X$ emissions originated from shipping, plus the NO$_X$ transported to OCN, and the influence of local photochemical reactions on O$_3$ is significant in OCN (38.7%)."

Comment 16: line 502 and Table 2: There is no citation for relevant studies of source-receptor relationship in South Korea and Japan. It is requested to be carefully reviewed other source-receptor studies. What is the consistency and/or difference from the result of this study?

Response: Thank you for your comments. We have added relevant references and analysis in the latest manuscript at line 527-530 as the blue text below:

"Long-term studies that analysed long-range transport of PM$_{2.5}$ seasonally or annually in South Korea and Japan reported that local contributions ranged from 30% to 60%, depending on the season, and local contribution was higher in the metropolises of Japan and South Korea (Kim et al., 2017; Yim et al., 2019; Lee et al., 2017). There is no significant difference between their studies and our results."

Comment 17: line 615 (caption of Table 3): "The median and range of the annual averages of the 6 models are given below." Is stated, but where is indicated? Is this statement mention on "reference" column?

Response: Thank you for your comments. The citation information in Table 3 is on page 167 of part A of the HTAP report (Dentener et al., 2010). The reference information has been stated at line 607-608 and has already mentioned on "reference" column. We are sorry to use the ambiguous expression of word "reference" in the table, and we have revised the table in the latest manuscript at line 640 as the blue text in the table below:

"**Table 3. Relative contributions (%) compared with those in the HTAP report (Dentener et al., 2010). The median and range of the annual averages of the 6 models are given below.**

	Receptor region*											
	EA			SA			EU			NA		
	HTAP	surface	PBL	HTAP	surface	PBL	HTAP	surface	PBL	HTAP	Surface	PBL
Nss-Sulphate:												
from EA	76.3 (72.5-87.0)	92.0	85.5	6.1 (1.9-9.6)	0.3	0.7	0.8 (0.0-1.6)	0.1	0.6	4.4 (0.0-5.3)	0.2	1.6
from SA	1.8 (1.5-3.2)	3.0	5.4	58.2 (50.3-71.9)	88.4	82.4	1.3 (0.0-6.8)	0.0	0.1	0.5 (0.0-0.7)	0.0	0.3
from EU	5.0 (0.3-9.8)	0.0	0.2	16.2 (12.1-22.1)	0.1	0.4	78.2 (66.5-91.0)	80.1	70.4	2.6 (0.8-4.6)	0.0	0.2
from NA	0.7 (0.1-2.5)	0.0	0.1	1.1 (0.3-3.5)	0.0	0.2	2.2 (1.1-4.6)	0.4	3.6	79.5 (69.0-83.9)	90.7	83.4
BC:												
from EA	84.6 (81.1-95.0)	94.0	81.0	4.8 (3.7-19.5)	0.1	1.1	1.0 (0.09-4.2)	0.0	1.5	2.7 (0.6-4.9)	0.0	5.7
from SA	2.9 (1.7-5.8)	2.3	6.0	71.3 (57.2-90.6)	95.0	73.6	1.2 (0.5-11.1)	0.0	0.7	0.7 (0.09-2.8)	0.0	1.8
from EU	1.0 (0.5-3.9)	0.0	0.3	4.3 (3.2-10.6)	0.0	1.0	88.7 (76.7-96.6)	93.5	64.9	1.4 (0.2-6.1)	0.0	0.3
from NA	0.2 (0.02-0.5)	0.0	0.2	0.5 (0.04-0.8)	0.0	0.5	1.1 (0.2-2.1)	0.0	6.7	79.1 (54.5-98.2)	96.5	70.5

* Note that there are some different definitions between the regions used in the table heading and in our study. The definitions of the regions in the table are stipulated by HTAP. Approximately, EA in HTAP is equal to EA in this paper, SA to SAS, EU to EUR, and NA to NAM."

Comment 18: Even though this manuscript entitled "source-receptor model", the discussion in the result of source-receptor relationship with other relevant studies are immature. As we can follow

from the configuration presented in Eq. (3), the tagged method will trace the geographical location where produced. This study presented the global-scale source-receptor relationships; however, how can we understand the air pollutants' production during long range transport? The presented Figure 14 shows large impact by "OCN" source for O_3. For example, NAM was dominated approximately 20% by OCN. In this case, where this O_3 transported from and produced? As seen from Figure 15, the contribution of EA is penetrated in NAM region; therefore, direct transport of O_3 produced over EA and additional O_3 impact produced over Pacific ocean could be found over NAM? If this is true, EA posed only 3.6% contribution over NAM but EA should be considered important source over NAM. Despite this large contribution by OCN, discussion was insufficient. Ultimately, how can we apply this OCN impact on policy making?

Response: Thank you for your valuable comments. Our S-R module can quantify the contributions of primary and secondary air pollutants from various source regions at the same time in one simulation. Primary pollutants are tagged by the emitting locations, and secondary aerosols are tagged by their precursor emitting locations because all their components are directly related to specific precursor species. For other secondary species, e.g., O_3, is tagged by the produced locations because its production relates to hundreds and thousands of reactions and its precursor relates to NO_x and hundreds of VOCs. It could lead to certain uncertainties when we tag precursor emitting locations of O_3. Therefore, for aerosols, we have already considered their production during long range transport, but for O_3, we have considered the amounts O_3 produced in source region which is direct transport and have neglected the quantities of O_3 produced during long range transport, that is, O_3 produced inside a source region from precursors emitted in neighboring source regions and transported to that source region. For example, in our study, OCN contributed about 19.5% to surface O_3 concentration in NAM and this O_3 produced in OCN and transported to NAM. EA contributed only 3.6% to NAM which means that O_3 produced in EA transports to NAM and makes a 3.6% contribution. It's lower than realistic transport contribution because many contributions has been attributed to OCN due to the precursors could transport to OCN under the control of westerly winds, react and produce O_3 on OCN. The 19.5% contribution of OCN includes the contribution of EA's precursors transported to OCN, NAM's precursors transported to OCN, and O_3 local produced due to precursors emitted from traffic source in OCN.

Based on the average of all grid cells in the receptor region, as shown in Fig. 8, we compute the contribution of source region EUR and EA transport to receptor region NAM and compare the results with Fiore et al. (2009) study which is cited in HTAP report. Except JJA and EA in DJF (black dots in Fig. 8), our results are within the range. Here we propose an indirect evaluation method to roughly estimate the maximum contribution of EA transport to NAM. Considering the NO_x from EA transported to OCN, we find a location where EA's contribution to surface NO_x in

OCN decreases and starts to be lower than 5%, then OCN local contributions to surface O_3 in the west of this location are all simply attributed to EA due to the precursor emitted in EA and transport to OCN. We compute the attenuation rate of O_3 transported from EA to NAM, then estimate how much O_3 that produced in OCN from precursors emitted in EA and transported to OCN can transport to NAM. The total contribution of this indirect transport and EA direct transport are considered as real contribution of EA to NAM. The new results are shown in Fig. 8 as purple dots. It can be seen that this evaluation method could influence S-R relationships a lot in DJF and MAM, and is around 1 ppb higher than the upper limit of Fiore et al. (2009). In fact, due to the traffic source in OCN and some natural emissions in OCN, the NO_x contribution standard of 5% from EA standard we select is lower, which means the results marked as purple dots are the maximum contribution from EA to NAM.

Moreover, due to the short lifetime of NO_x, most NO_x in OCN is from their local and natural emissions. As shown in Fig. 9, although the production rate of O_3 in OCN is lower than that in continents, it cannot be ignored, especially in the deep ocean aeras where NO_x cannot be transported from EA. Therefore, emissions from OCN also need to be controlled.
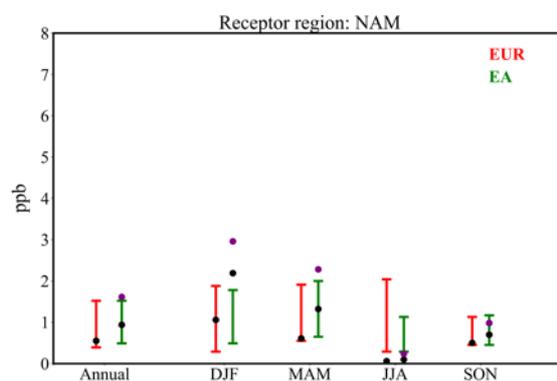
Figure 8. Annual and seasonal mean contribution to NAM surface O_3 from EUR and EA. (red vertical bars for EUR, green vertical bars for EA (Fiore et al., 2009), black dots for our results, purple dots for our new approach results). The contributions from Fiore et al. (2009) are estimated by linearly scaling the simulated surface O_3 response to the combined 20% decreases in anthropogenic emissions of NO_x, CO, and NMVOC in the source regions to 100% decreases.
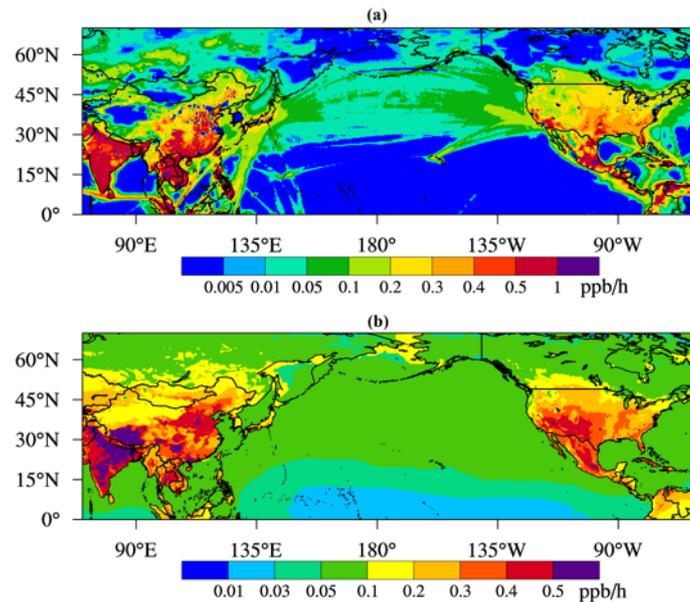
Figure 9. (a) annual net O₃ production rate; (b) removal of O₃ by dry deposition.

We have revised it in the latest manuscript at line 543-548 as the blue text below:

"Different from $PM_{2.5}$, O_3 S-R relationships are affected by many precursors that are emitted, reacted, and then generated, which are also attributed to the influence of photochemical reactions, and show a stronger nonlinearity. In our S-R module, primary pollutants and secondary aerosols are tagged by their or their precursor emitting locations, and other secondary species like O_3 are tagged by the produced locations. Therefore, we calculate the O_3 contribution of a source region that was chemically produced inside this source region and then transported to another receptor region, inevitably including amounts of O_3 produced inside this source region from precursors emitted in neighboring source regions and transported to this source region."

Referee #2:

Comment 1: P. 2, L. 58: Does "research area of observations" means coverage areas of field observations?

Response: Thank you for your comments. Yes. The "limited research area of observations" at line 58 means that the research area covered by field observation activities is always limited.

Comment 2: P.2-3, third paragraph in Introduction section: This paragraph describes background information on S-R calculation methods and model resolution impacts on model performance and is mix of distinct topics. For readability, these topics need to be separated in individual paragraph.

Response: Thank you for your valuable comments. We have separated this paragraph into three paragraphs in the latest manuscript.

Comment 3: P. 2, L. 63-64: Klich and Fuelberg (2014) is not global modeling study. Please add the appropriate reference.

Response: Thank you for your comments. We have changed this reference and have added the appropriate references in the latest manuscript at line 64 as the blue text below:

   "Many global chemical transport models have been used to study the distribution of air pollutants and estimate their intercontinental transport (Wai et al., 2016; Yang et al., 2017)."

Comment 4: P. 5, L. 134: What does "sensitivity analysis" mean?

Response: Thank you for your comments. As described in line 65, sensitivity analysis, "it mainly refers to the reduction in emissions in the source region by a certain extent, such as 15% or 20%, or even directly returning to zero." Because for primary pollutants, such as BC, their S-R relationships are nearly linear and are different from secondary pollutants, such as O_3. The neglect of nonlinear error in sensitivity analysis has much less impact on the results of S-R relationships of primary pollutants. To better understand the "sensitivity analysis" method here, we have revised it in the latest manuscript at line 137 as the blue text below:

   ", so emission sensitivity analysis can provide an accurate S-R assessment."

Comment 5: P. 7, L. 192: Why do authors choose the year 2018 for simulation, even though emission for 2015 were used?

Response: Thank you for your valuable comments. We choose the year 2018 for simulation because we have more observation data in China in 2018 and China have completed the toughest-ever clean air policy, where BC, NO_x, primary $PM_{2.5}$, SO_2 emissions have all significantly decreased due to the implementation of the policy. Zhang et al. (2019) reported that from 2015 to 2017 SO_2 emissions in

China decreased by 35%, while NO_x and NMVOC emissions changed slightly with a decrease lower than 10%. However, this significant SO_2 change is not reflected in most emission inventories, which should lead to uncertainties on the S-R relationships, e.g., it could be a possible reason for the overestimation of SO_2 in China and may have an impact on our analysis of nss-sulphate transport from China to the downwind regions in our study. As for using different years of emission inventories in this simulation, the official inventories made by countries or regions have at least a 1-year time lag (Janssens-Maenhout et al., 2015), and the global emission inventories, e.g., EDGAR has a nearly 5-year time lag and is currently updated to year 2015. In order to understand the possible influence on inconsistent inventory years on the results, we compared the 1-year change rate of pollutants emissions in three regions (NAM, EUR, China) as shown in Fig. 1. The 1-year change rate of BC in NAM ranges around $\pm 10\%$ and in EUR ranges within $\pm 5\%$. BC emissions in China have changed within $\pm 10\%$ since 2010. The 1-year change rate of primary $PM_{2.5}$ in three regions are all within $\pm 10\%$. The 1-year change rate of NO_x and SO_2 in three regions ranges within $\pm 5\%$ and $\pm 10\%$ since 2010, respectively. All change rates are within the region and pollutant emission uncertainties (95% confidence interval) reported by Crippa et al. (2019). For example, the SO_2 emission uncertainty in China, USA, Canada is 12%, 31%, 53%, respectively. NAM refers to USA and Canada. Moreover, from the perspective of the 3-year change rate, global total emissions changed a little within $\pm 5\%$ between 2015 and 2012. We also computed the annual BC, SO_2, CO emissions in year 2017, 2018, 2019 from the Community Emissions Data System (CEDS) for Historical Emissions, their 1-year change rate of BC, SO_2 and CO ranges from -1.6% to -0.6%. It can be seen that there is no significant change of emission inventories between 2015 and 2018, and we have more observation data in China in 2018. Therefore, we chose the emission inventory 2015 to simulate the year 2018.

Figure. 1 Annual emissions and 1-year change rate of BC, NOₓ, primary PM₂.₅ and SO₂ in (a) NAM, (b) EUR, and (c) China from 2001 to 2015.

Comment 6: P. 7, Section 2.4: Please clarify treatments of soil NOₓ emissions and volcanic SO₂ emissions in the simulation.

Response: Thank you for your valuable comments. In our model, the soil NOₓ emissions are from Global hourly emissions for soil NOₓ (Hudman et al., 2012; data available at http://ftp.as.harvard.edu/gcgrid/data/ExtData/HEMCO/OFFLINE_SOILNOX/v2019-01/), and the volcanic SO₂ emissions are from Carn et al. (2015) (data available at http://ftp.as.harvard.edu/gcgrid/data/ExtData/HEMCO/VOLCANO/v2019-08/). We have added it in the latest manuscript at line 217-220.

Comment 7: P. 11, L. 283-284: "In the model, stratospheric O₃ is constrained by relaxation towards zonally and monthly averaged values from ozone climatologies from Logan (1999)." Is it consistent with the description in section 2.3: "After calculation of tropospheric height, the monthly stratospheric ozone above the troposphere is taken from the climatic mean output from MOZART v2.4 (Horowitz et al., 2003)." (P. 7, L. 194-195)?

Response: Thank you for your valuable comments. These two descriptions are consistent. The Horowitz et al. (2003) study where we referred the treatment method also used original values from

ozone climatologies from Logan (1999) in stratospheric O_3. Therefore, two references we both added in our manuscript. We have cited these two references at two sentences in the latest manuscript.

Comment 8: P. 11, L. 286: "The coarse vertical resolution…" What vertical resolutions do the GNAQPMS have in the UTLS regions? Are these errors introduced by model physical processes or tracer advection scheme?

Response: Thank you for your comments. In the vertical direction, we divide 20 layers. The bottom layer is about 50 m and the top layer is about 20 km. About 6 layers are located above 6 km. As you said, these errors may introduce by model physical processes. The inadequate resolution of the tropopause and excessive cross-tropopause transport of O_3 in the model could result in the overestimation of O_3. The top boundary of O_3 in our model are referred from Horowitz et al. (2003). The vertical direction is divided into 34 layers extending up to 4hPa in Horowitz et al. (2003), and the model they used tends to overestimate O_3 in the vicinity of the tropopause by 25% or more. Similar reasons have also been pointed out that inadequate resolution of tropopause location and excessive production of O_3 in the UTLS regions are responsible for the overestimation. Above 15 km, we only divide 3 layers and it's relatively coarse. In the horizontal direction, our resolution is 0.5°, which is sufficient that Eastham and Jacob (2017) has reported that 1° is sufficient. Wei et al. (2019) computed the global budgets and proved global mass conservation of model which used the same advection scheme with us, so the advection scheme should not have much influence on our overestimation.

Comment 9: P. 11, L. 290-292: "Note that the model overestimation in the upper troposphere does not affect our analysis of surface O_3 and its origins because O_3 in the upper troposphere has little effect on the surface O_3 concentration." Is it confirmed by authors' tagged tracer calculation?

Response: Thank you for your comments. This statement is imprecise and mainly focuses on the mid-latitude continent in the Northern Hemisphere. Compared with the contribution of photochemical reactions, stratosphere is not the major contributor in the main continents in the Northern Hemisphere. We select 4 stations, Resolute, Hilo, Hohenpeissenberg and Sapporo. Resolute and Hilo are located in NAM; Hohenpeissenberg is located in EUR; Sapporo is located in EA. The transport from stratosphere can reach a peak of around 10 ppb to surface concentration in DJF, with relative contribution lower than 20%. Their seasonal contributions of top boundary are compared with Sudo and Akimoto (2007) results as shown in Fig. 2. Sudo and Akimoto (2007) simulation captures the variation of O_3 in the upper troposphere and stratosphere well. Although our results overestimate the contribution, it's still within an acceptable range, with R value 0.67, NMB

value 33% and FAC2 value 72.9%. We also capture the seasonal variation of stratosphere contribution. However, we have to admit that according to the results of S-R relationships, the Southern Hemisphere is greatly affected by stratospheric transport, and this overestimation will inevitably overestimate the transport from stratosphere. We have deleted this sentence in the latest manuscript.
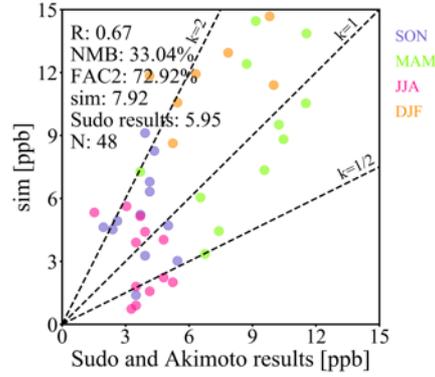
Figure 2. Scatterplots of simulated (sim) and Sudo and Akimoto (2007) seasonal stratosphere contributions to O$_3$ at 4 stations. The black dotted lines are the 2:1, 1:1, and 1:2 reference lines from left to right. Different seasons are plotted with circles in different colors.

Comment 10: P. 13, Section 3.1.3: There are no explanation how authors compare the model results with TROPOMI tropospheric NO$_2$ data (e.g., spatial and temporal sampling from model outputs, application of averaging kernels).

Response: Thank you for your comments. The horizontal resolution of our simulation is 0.5°×0.5° and the resolution of TROPOMI data is 0.125°×0.125°. The column of NO$_2$ (DU) is computed as follows:

$$DU = \sum\nolimits_{i=1}^{n} \frac{plev_i \times conc_i \times 100 \times 6.02 \times 10^{23}}{8.34 \times T_i \times 10^{13}} \times dz_i$$

where $plev_i$, $conc_i$, T_i, dz_i are pressure, concentration of NO$_2$, temperature and height of the ith layer, respectively.

The Tropospheric Monitoring Instrument (TROPOMI) was loaded onboard the Sentinel-5 satellite for fine gas monitoring and the TROPOMI NO$_2$ data retrieval is described in the product Algorithm Theoretical Basis Document (van Geffen et al., 2020). The monthly tropospheric NO$_2$ column concentration data from the Royal Netherlands Meteorological Research Institute (KNMI) used in our paper has measurement loss in some areas. We compared the NO$_2$ columns through one-by-one correspondence between the simulation time and the TROPOMI data observed time, the model grid cell and TROPOMI data grid cell. The simulation results (DU) when drawing, are filled with model results if the grid cell misses measurement in the TROPOMI data. In order to be consistent, in the latest manuscript we have eliminated the grid cells in our simulation which is missing in the

TROPOMI data as shown in Fig. 3 below.
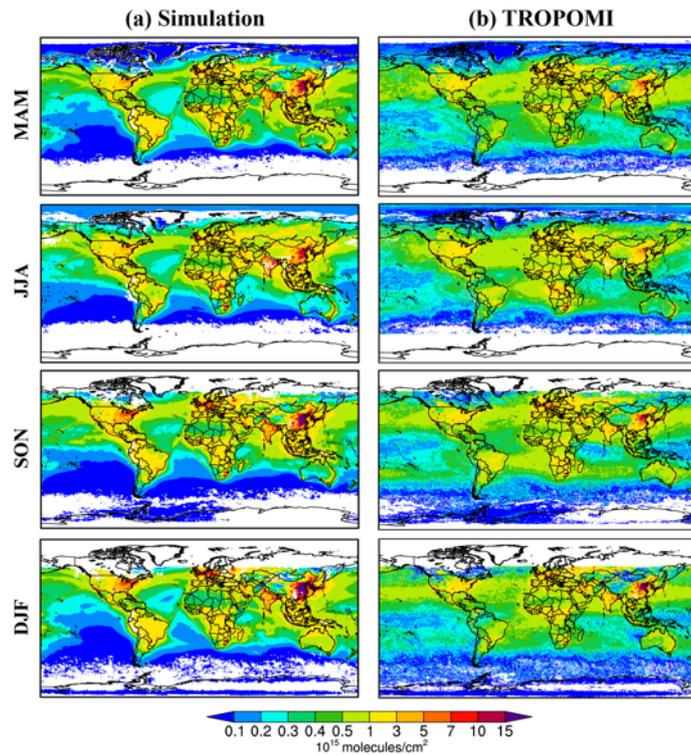
Figure 3. Spatial distributions of seasonal mean NO₂ columns from (a) GNAQPMS averaged in 2018 and (b) the TROPOMI data.

We have added these descriptions in the latest manuscript at line 250-258 as the blue text below:

"NO₂ columns are compared with tropospheric NO₂ column concentration data from the Tropospheric Monitoring Instrument (TROPOMI; van Geffen et al. (2020); data available at http://www.temis.nl/airpollution/no2.php), and the resolution of monthly TROPOMI NO₂ data from the Royal Netherlands Meteorological Research Institute (KNMI) used in our paper is 0.125°×0.125°. … … We compared the spatial distribution of AOD and NO₂ columns through one-by-one correspondence between the simulation time and the MODIS, TROPOMI observed time, the model grid cell and MODIS, TROPOMI data grid cell."

Comment 11: P. 13, Section 3.1.3: TROPOMI low biases (Verhoelst et al., 2021) may also be possible reason for model positive biases.

Response: Thank you for your valuable suggestions. We have added this possible reason in the latest manuscript at line 339-340 as the blue text below:

"A negative bias for TROPOMI satellite data compared to the ground-based measurements (Verhoelst et al., 2021) may also be a reason for our model positive biases."

Comment 12: P. 14, L. 330-331: "since there is higher biomass and fossil fuel burning for heating

during DJF" Do seasonal cycles of precipitation affect seasonal cycles of simulated PM$_{2.5}$ concentrations?

Response: Thank you for your comments. The removal of pollutants from the atmosphere can occur in one of two ways: by wet deposition or dry deposition. Wet deposition is the process of washing out pollutants from the air by precipitation or cloud droplets. Seasonal cycles of precipitation will affect wet deposition, and then affect seasonal cycles of simulated PM$_{2.5}$ concentration. The simulated precipitation field is shown in Fig. 4. The PM$_{2.5}$ concentration in major PM$_{2.5}$ hotspots India, East Asia, and Central Africa reaches a peak during DJF and a trough in JJA. Similarly, the precipitation reaches a maximum in JJA and a minimum in DJF in these regions, which is corresponding to the wet deposition peak in JJA. Moreover, the Planetary Boundary Layer (PBL) plays an important role by exchanging heat and moisture between the surface and free atmosphere. A high concentration of PM$_{2.5}$ will enhance the stability of PBL, which in turn decreases the PBL height. Lower PBL height is associated with weaker turbulence mixing, leading to favorable conditions for the accumulation of air pollutants in the shallow PBL and this positive feedback mechanism will strengthen in DJF (Petaja et al., 2016; Yin et al., 2019).
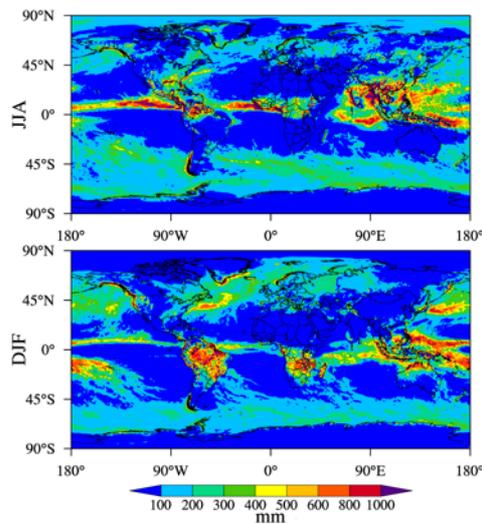
Figure 4. Simulated seasonal precipitation in JJA and DJF.

We have updated these reasons in the latest manuscript at line 349 as the blue text below:

", and the lowest values are during JJA and SON since there is higher biomass and fossil fuel burning for heating, less precipitation and strengthened positive feedback between aerosols and PBL (Petaja et al., 2016) during DJF."

Comment 13: P. 16, L. 383: What is the definition of "SNA"?

Response: Thanks for your comments. As described at line 260, SNA "refers to the sum of sulphate, nitrate and ammonium".

Comment 14: P. 17, L. 389: "heterogeneous chemistry on aerosol surfaces" Please add the references which support this speculation.

Response: Thank you for your comments. We have added the appropriate references to support at line 407 as the blue text below:

  "heterogeneous chemistry on aerosol surfaces (Bauer and Koch, 2005; Andreae and Crutzen, 1997)"

Comment 15: P. 17, L. 401: "a trough in DJF" Is this trough over eastern China also influenced by NO_x titration?

Response: Thank you for your valuable comments. We compared the seasonal spatial distribution of NO and NO_2 as shown in Fig. 5. Surface NO and NO_2 over eastern China reaches a maximum in DJF and SON and a minimum in MAM and JJA, which is opposite from the surface O_3 concentration. The O_3 trough in DJF at urbanized eastern China could be due to the enhanced O_3 titration effect by the increase of NO_x. We have added this possible reason in the latest manuscript at line 420-421 as blue text below:

  ", and this seasonality is determined by abundant photochemical reactions in JJA and the East Asian monsoon. The enhanced titration of O_3 by the increased NO_x in DJF could also be a possible reason."
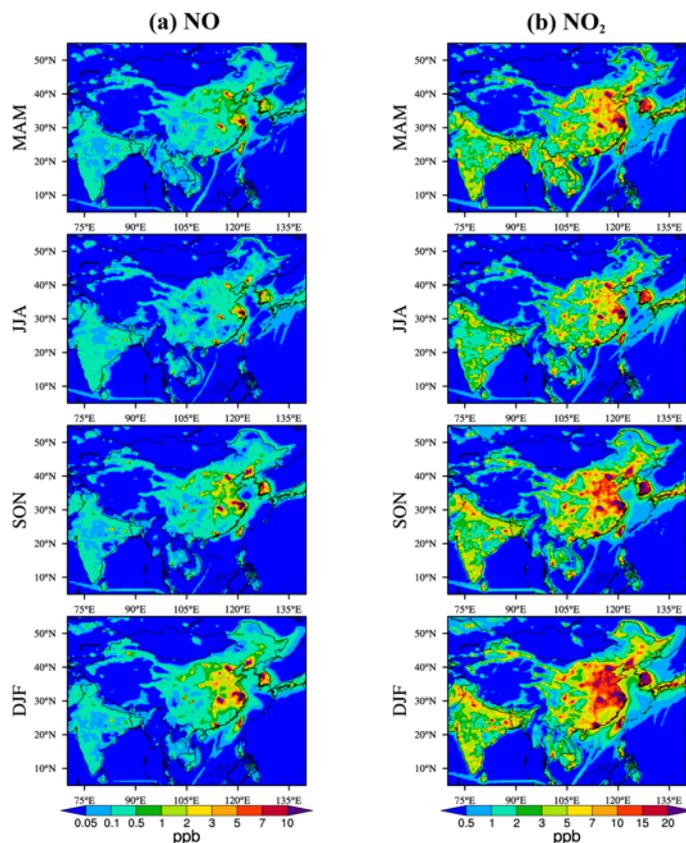
Figure 5. Spatial distributions of seasonal mean (a) NO and (b) NO_2 surface concentrations.

Comment 16: P. 18, Figure 8: What is a possible reason why model PM$_{2.5}$ biases are larger in MAM than in other seasons?

Response: Thank you for your comments. Seasonally, 72.85% of all dust storms occurred in the spring (MAM), 16.39% in winter (DJF), 8.71% in summer (JJA), and 2.05% in autumn (SON) in northern China (Deng et al., 2013). Many studies have stated that the mechanism for the outbreak and development of dust storms are not yet fully understood and the techniques for local dust storm in China forecasting require further improvement (Huang et al., 2006; Sun et al., 2006; Wang et al., 2019). Therefore, the larger PM$_{2.5}$ biases in MAM may be due to the spring dust storms over northern China, which is difficult to simulate, e.g., several stations underestimated and circled by the red box in Fig. 6. We have added this reason in the latest manuscript at line 437-438 as the blue text below:

"The model shows good spatial correlations with observations and little seasonal bias, with R values ranging from 0.91-0.92 and NMB values within ±15%. The frequent spring dust storms in northern China are an important reason for the larger PM$_{2.5}$ biases in MAM."
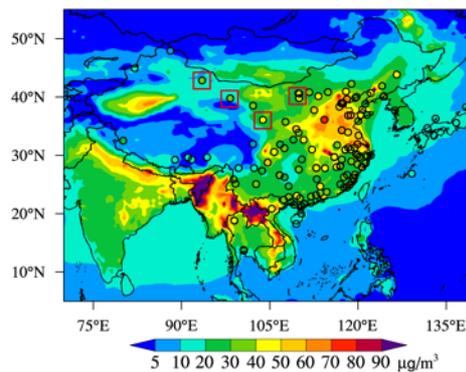
Figure 6. Spatial distribution of simulated (shaded) surface PM$_{2.5}$ concentrations compared with observations (solid circles) in MAM in East Asia.

Comment 17: P. 19, Figure 9: This figure shows "Validation of GNAQPMS simulations against EMEP observations."

Response: Thank you for your comments. We have revised this sentence in the latest manuscript at line 448 as the blue text below:

"Figure 9 shows the validation of GNAQPMS simulations against EMEP observations."

Comment 18: P. 23, L. 467: The title of section 4 is confusing. Section 3 also contains results of this study.

Response: Thank you for your comments. We have changed the title of section 4 to "Results of S-

R relationships" in the latest manuscript at line 487.

Comment 19: P. 23, L. 472: How do biogenic secondary organic aerosols account for?

Response: Thank you for your comments. Biogenic secondary organic aerosols are considered to be from natural emission sources.

Comment 20: P. 27, L. 537: ", while the contribution of the top boundary is small in other receptor regions and …" Is it correct? In Figure 14, "Boundary" have second or third most contributions in most receptor regions.

Response: Thank you for pointing out our imprecise express. Sources of O_3 to the troposphere include downward transport from the stratosphere (Junge, 1962) and photochemical production from precursors (Monks et al., 2009). The smaller contribution of the top boundary is relative to the contribution of photochemical reactions. We have revised it in the latest manuscript at line 565-566 as the blue text below:

   "The contribution of the top boundary is large in SPO due to the low tropopause of SPO and the simplified treatment of the stratosphere, while the contribution of the top boundary is smaller in Northern Hemisphere receptor regions compared with the contribution of photochemical reactions."

Comment 21: P. 28, Section 4.2: Why do authors evaluate S-R relationships of BC and sulfate in the PBL only in this section?

Response: Thank you for your careful comments. First, the S-R relationships of $PM_{2.5}$ and O_3 in the surface layer have already been briefly analyzed in section 4.1, and we hope to show the advantage that our model can quantify the contributions of multiple air pollutants from various source regions at the same time in one simulation. Secondly, BC as the representative of primary aerosol and sulphate as the representative of secondary aerosol both make a great influence on our environment and climate. They tend to play opposite roles in their radiative effects. While sulphate is characteristic of strong radiation scattering and thus leads to a cooling surface (negative radiative forcing), BC heats up the atmosphere owing to its excellent ability of absorbing solar radiation. It's important to analyze their S-R relationships. In addition, due to the limitation of manuscript length, our purpose is to introduce the added S-R module, which can help us analyze the S-R relationships of pollutants, rather than discussing the results of each tagged pollutant in detail. Therefore, we only evaluate S-R relationships of BC and sulfate in section 4.2.

Comment 22: P. 33, L. 673: Vertical resolution is also important for resolving intercontinental transport plumes (Eastham and Jacob, 2017). Do authors plan to investigate the sensitivity of S-R

relationships to different vertical resolutions?

Response: Thank you for your valuable suggestions which really provide a great thinking direction. As Eastham and Jacob (2017) stated, the inadequate vertical grid resolution cannot properly resolve plume gradients. We have already divided the vertical layer into 40 layers to better analyze the S-R relationships, although this new vertical resolution is much coarser compared with a vertical resolution of 100 m in the free troposphere. About 20 layers are located above 3km and about 12 layers are located above 6 km. We will incorporate this into our future plans. It's a great question worthy of careful discussion. We have added this sentence in the latest manuscript at line 652-653 as the blue text below:

"The inadequate vertical grid resolution cannot properly resolve plume gradients which could also introduce uncertainties (Eastham and Jacob, 2017)."

Comment 23: Authors emphasize advantages of S-R calculation in their models (i.e., tagged tracer method) over sensitivity simulation analyses with perturbed emissions on the aspects of errors introduced from non-linear chemistry and computational resources in abstract, introduction, and summary. I generally agree them, whereas I miss more detailed analysis and discussion of effects of differences in S-R calculation methods. For example, the HTAP-like sensitivity simulations using GNAQPMS-SM in which emissions are perturbed for a few key regions would help isolate the effects of S-R calculation methods from the effects of the other model representations (e.g., chemical and transport processes, horizontal resolution, emission inventories, etc.).

Also, authors compare their results of S-R relationship assessment for BC and sulfate aerosols with the HTAP report. Why do not authors compare S-R relationships of surface ozone with the HTAP report? I suppose that an impact of errors introduced from non-linear chemistry on ozone S-R relationship is larger than that on aerosol S-R relationships.

Response: Thank you for your constructive comments. Indeed, in addition to the different methods of studying the S-R relationships, the model, horizontal resolution, emission inventories we used are also different from HTAP used, which may bring some uncertainties when we compare their differences.

We try to do some comparisons on the two approaches. Taken O_3 as an example, emission sensitivity approach estimates intercontinental transport of surface O_3 resulting from 20% reductions of anthropogenic O_3 precursor emissions for each source region, and HTAP chose this method. It's attributable to the precursor emitting locations. In contrast, for O_3, it's tagged by the produced locations in our model because its production relates to hundreds and thousands of reactions and its precursor relates to NO_x and hundreds of VOCs. It could lead to certain uncertainties when we tag precursor emitting locations of O_3. Li et al. (2008) compared these two

methods for the contribution of high O_3 concentration regions in China and found that the difference could be as much as 30%.

Based on the average of all grid cells in the receptor region, we compute the contribution of source region EUR and NAM transport to receptor region EA and compare the results with Fiore et al. (2009) study which is cited in HTAP report. When extrapolated to a 100% source contribution, as shown in Fig. 8b, the Fiore et al. (2009) results suggest that EU and NA contribute from 0.5-2.8 ppb and 0.3-1.4 ppb to surface O_3 in EA in MAM and JJA, respectively. NAM's contribution to EA in our results are consistently lower, but the annual results are within the range given by other studies which Fiore et al. (2009) cited in their Fig. 11. There are many possible reasons for this difference. Their results are multi-model estimates and model horizontal resolution ranged from 5°×5° to 1° ×1°. The different methods are used. We have considered the amounts O_3 produced in source region which is direct transport and have neglected the quantities of O_3 produced during long range transport. For example, in our study, OCN contributed about 19.5% to surface O_3 concentration in NAM and this O_3 produced in OCN and transported to NAM. EA contributed only 3.6% to NAM which means that O_3 produced in EA transports to NAM and makes a 3.6% contribution. It's lower than realistic transport contribution because many contributions has been attributed to OCN due to the precursors could transport to OCN under the control of westerly winds, react and produce O_3 on OCN. The 19.5% contribution of OCN includes the contribution of EA's precursors transported to OCN, NAM's precursors transported to OCN, and O_3 local produced due to precursors emitted from traffic source in OCN. As shown in Fig. 8a, in receptor region NAM, although most of our results are within the range, we still underestimate the real contribution from EA to NAM. Here we propose an indirect evaluation method to roughly estimate the maximum contribution of EA transport to NAM. Considering the NO_x from EA transported to OCN, we find a location where EA's contribution to surface NO_x in OCN decreases and starts to be lower than 5%, then OCN local contributions to surface O_3 in the west of this location are all simply attributed to EA due to the precursor emitted in EA and transport to OCN. We compute the attenuation rate of O_3 transported from EA to NAM, then estimate how much O_3 that produced in OCN from precursors emitted in EA and transported to OCN can transport to NAM. The total contribution of this indirect transport and EA direct transport are considered as real contribution of EA to NAM. The new results are shown in Fig. 8a as purple dots. It can be seen that this evaluation method could influence S-R relationships a lot in DJF and MAM, and is around 1 ppb higher than the upper limit of Fiore et al. (2009). In fact, due to the traffic source in OCN and some natural emissions in OCN, the NO_x contribution standard of 5% from EA standard we select is lower, which means the results marked as purple dots are the maximum contribution from EA to NAM.
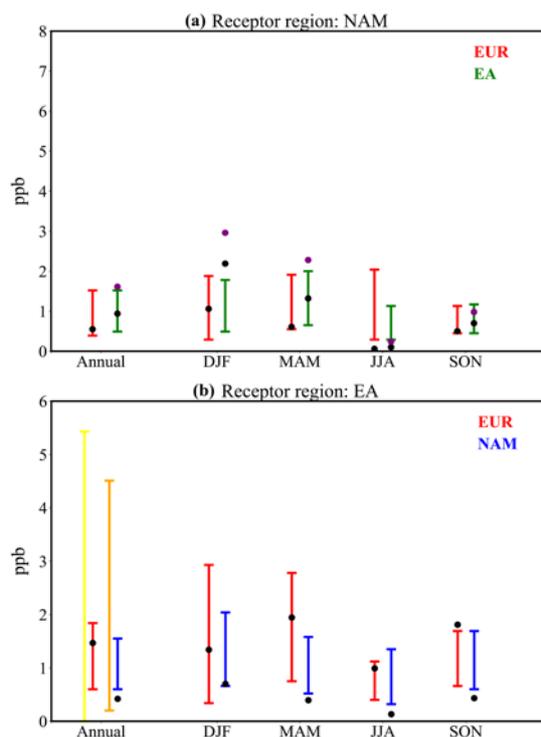
Figure 8. Annual and seasonal mean contribution to NAM and EA surface O$_3$ from source regions. (red vertical bars for EUR, blue vertical bars for NAM, green vertical bars for EA (Fiore et al., 2009); yellow vertical bars for EUR, orange vertical bars for NAM but from other studies which Fiore et al. (2009) cited in their Fig. 11; black dots for our results, purple dots for our new approach results). The contributions from Fiore et al. (2009) are estimated by linearly scaling the simulated surface O$_3$ response to the combined 20% decreases in anthropogenic emissions of NO$_x$, CO, and NMVOC in the source regions to 100% decreases.

We have added the comparison about surface O$_3$ in the latest manuscript at line 643-647 as the blue text below:

"We also compare the contributions to receptor region NAM and EA surface O$_3$ with Fiore et al. (2009) study which is related to HTAP report studies as shown in Fig. S3. When extrapolated to a 100% source contribution, the Fiore et al. (2009) results suggest that EUR and EA contribute from 0.3-2.1 ppb and 0.3-2.0 ppb to surface O$_3$ in NAM and EUR and NAM contribute from 0.4-2.9 ppb and 0.3-2.0 ppb to surface O$_3$ in EA, respectively. Although most of our results are within the range, NAM's contribution to EA in our results are consistently lower, and the contributions from EUR and EA to NAM are lower in JJA."

As you suggested, we have carried out additional emission sensitivity simulations and added some discussions in the latest manuscript at line 660-682 as the blue text below:
"

4.4 Comparison with emission sensitivity simulation results
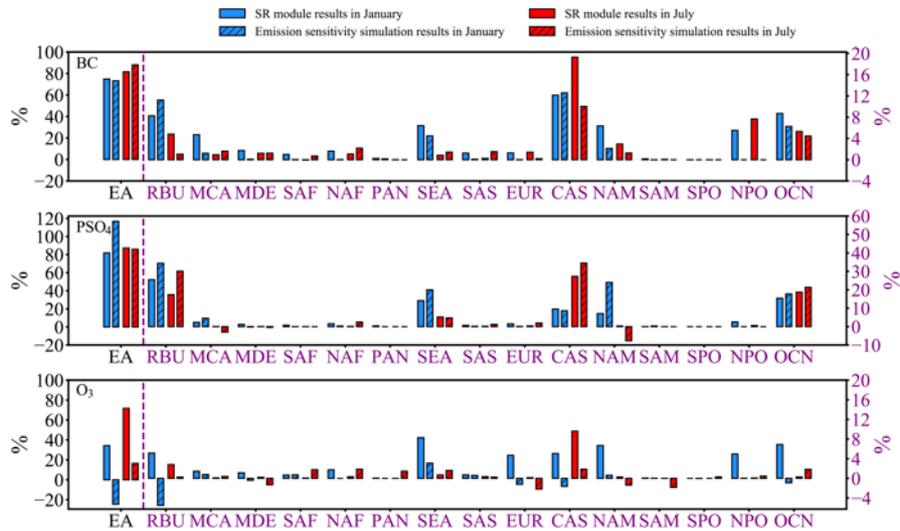
Figure 18. BC, nss-sulphate within the PBL and surface O₃ contribution from SR module results and full response from emission sensitivity simulation results from EA source region in January and July. The Y-axis of receptor region EA is the coordinate axis on the left shown in black, and the Y-axis of other receptor regions is the coordinate axis on the right shown in purple.

EA is an emission hot spot in the world. To better isolate the S-R calculation methods' effects of other possible reasons, e.g., horizontal and vertical resolution, emission inventories, models, we have carried out an additional emission sensitivity simulation with 20% reduction of anthropogenic emissions in EA in January and July of 2018. Pollutant response is defined as the ratio between the concentration difference between the baseline scenario and the perturbation scenarios and the concentration of the baseline scenario, based on the average of all grid cells in the receptor region. We make the hypothesis that −20 % perturbation responses can be extrapolated towards -100% perturbation range, as an approximation of full response from the source region EA and compare with our SR module results as shown in Fig. 18. The SR module results are consistently higher than the emission sensitivity simulation results, except in few regions, partly reflecting the SR module method pays attention to all global sources instead of anthropogenic component from regions we focus on, the conclusion of which is consistent with HTAP report (Dentener et al., 2010). There is no significant difference on BC, suggesting that BC levels are largely driven by local emissions and long-range transport. Nss-sulphate and O₃ responses exist negative values, suggesting that regional nss-sulphate and O₃ levels are also driven by precursor emissions besides local emissions and long-range transport. Compared with O₃, the difference between two methods on nss-sulphate is smaller. O₃ shows more negative response and larger difference. Especially in receptor region EA in January, the O₃ response are negative due to the strong non-linearity in O₃ chemistry. In our SR module method, all contributions are strictly positive. However, in emission sensitivity method, the impacts

are computed and may appear negative values, particularly in higher emission regions in DJF, which is also reported in Li et al. (2008) and Grewe (2004). The differences between two S-R revealing methods in estimated S-R relationships of secondary aerosols and O_3 are mainly due to the ignorance of the nonlinearity of pollutants during chemical processes."

Besides changes mentioned above, we also made some changes in the latest manuscript. These changes will not influence framework of the paper. The changes are simply listed as following:

1) In abstract, we deleted the sentence "In this study, local contributions to surface nss-sulphate and BC exceed the ranges given in the HTAP model, while local contributions to nss-sulphate and BC within the PBL are mainly within the ranges." We added the sentence "Additional emission sensitivity simulation shows a negative O_3 response in receptor region EA in January from EA. The difference between two methods in estimated S-R relationships of nss-sulphate and O_3 are mainly due to ignoring the nonlinearity of pollutants during chemical processes."

2) In summary at line 722-724, we added the sentence "Compared with Fiore's results, most of our results are within the range, except that NAM's contribution to EA surface O_3 in our results are consistently lower, and the contributions from EUR and EA to NAM surface O_3 are lower in JJA."

3) In summary at line 732-736, we added the sentence "Additional emission sensitivity simulation shows a negative O_3 response in receptor region EA in January from EA. The difference between two S-R revealing methods in estimated S-R relationships of secondary aerosols and O_3 are mainly due to ignoring the nonlinearity of pollutants during chemical processes. The SR module results are consistently higher than the emission sensitivity simulation results, except in few regions, partly reflecting the SR module method pays attention to all global sources instead of anthropogenic component from regions we focus on."

We appreciate for your positive comments and valuable suggestions to improve the quality of our manuscript.

On behalf of all the co-authors, best regards,

Qian Ye

Andreae, M. O.: Climatic effects of changing atmospheric aerosol levels, in: Future climates of the world: a modelling perspective, World Survey of Climatology, 347-398, 1995.

Andreae, M. O., and Crutzen, P. J.: Atmospheric aerosols: Biogeochemical sources and role in atmospheric chemistry, Science, 276, 1052-1058, 10.1126/science.276.5315.1052, 1997.

Bauer, S. E., and Koch, D.: Impact of heterogeneous sulfate formation at mineral dust surfaces on aerosol loads and radiative forcing in the Goddard Institute for Space Studies general circulation model, Journal of Geophysical Research-Atmospheres, 110, 15, 10.1029/2005jd005870, 2005.

Carn, S. A., Yang, K., Prata, A. J., and Krotkov, N. A.: Extending the long-term record of volcanic SO2 emissions with the Ozone Mapping and Profiler Suite nadir mapper, Geophys. Res. Lett., 42, 925-932, 10.1002/2014gl062437, 2015.

Crippa, M., Janssens-Maenhout, G., Guizzardi, D., Van Dingenen, R., and Dentener, F.: Contribution and uncertainty of sectorial and regional emissions to regional and global PM2.5 health impacts, Atmospheric Chemistry and Physics, 19, 5165-5186, 10.5194/acp-19-5165-2019, 2019.

Deng, H., Jiang, W. F., Chen, Y. Y., and Shu, S. G.: The temporal and spatial distribution of dust storms on the North China Plain, AD 1464-1913, Holocene, 23, 625-634, 10.1177/0959683612467479, 2013.

Dentener, F., Keating, T., and Akimoto, H.: Hemispheric Transport of Air Pollution 2010, United Nations, 2010.

Eastham, S. D., and Jacob, D. J.: Limits on the ability of global Eulerian models to resolve intercontinental transport of chemical plumes, Atmospheric Chemistry and Physics, 17, 2543-2553, 10.5194/acp-17-2543-2017, 2017.

Fiore, A. M., Dentener, F. J., Wild, O., Cuvelier, C., Schultz, M. G., Hess, P., Textor, C., Schulz, M., Doherty, R. M., Horowitz, L. W., MacKenzie, I. A., Sanderson, M. G., Shindell, D. T., Stevenson, D. S., Szopa, S., Van Dingenen, R., Zeng, G., Atherton, C., Bergmann, D., Bey, I., Carmichael, G., Collins, W. J., Duncan, B. N., Faluvegi, G., Folberth, G., Gauss, M., Gong, S., Hauglustaine, D., Holloway, T., Isaksen, I. S. A., Jacob, D. J., Jonson, J. E., Kaminski, J. W., Keating, T. J., Lupu, A., Marmer, E., Montanaro, V., Park, R. J., Pitari, G., Pringle, K. J., Pyle, J. A., Schroeder, S., Vivanco, M. G., Wind, P., Wojcik, G., Wu, S., and Zuber, A.: Multimodel estimates of intercontinental source-receptor relationships for ozone pollution, Journal of Geophysical Research-Atmospheres, 114, 21, 10.1029/2008jd010816, 2009.

Grewe, V.: Technical Note: A diagnostic for ozone contributions of various NOx emissions in multi-decadel chemistry-climate model simulations, Atmospheric Chemistry and Physics, 4, 729-736, 10.5194/acp-4-729-2004, 2004.

Guanter, L., Aben, I., Tol, P., Krijger, J. M., Hollstein, A., Kohler, P., Damm, A., Joiner, J., Frankenberg, C., and Landgraf, J.: Potential of the TROPOspheric Monitoring Instrument (TROPOMI) onboard the Sentinel-5 Precursor for the monitoring of terrestrial chlorophyll fluorescence, Atmospheric Measurement Techniques, 8, 1337-1352, 10.5194/amt-8-1337-2015, 2015.

Hand, J. L., Gill, T. E., and Schichtel, B. A.: Spatial and seasonal variability in fine mineral dust and coarse aerosol mass at remote sites across the United States, Journal of Geophysical Research-Atmospheres, 122, 3080-3097, 10.1002/2016jd026290, 2017.

Horowitz, L. W., Walters, S., Mauzerall, D. L., Emmons, L. K., Rasch, P. J., Granier, C., Tie, X. X., Lamarque, J. F., Schultz, M. G., Tyndall, G. S., Orlando, J. J., and Brasseur, G. P.: A global simulation of tropospheric ozone and related tracers: Description and evaluation of MOZART, version 2, Journal of Geophysical Research-Atmospheres, 108, 29, 10.1029/2002jd002853, 2003.

Horowitz, L. W., Naik, V., Paulot, F., Ginoux, P. A., Dunne, J. P., Mao, J. Q., Schnell, J., Chen, X., He, J., John, J. G., Lin, M. Y., Lin, P., Malyshev, S., Paynter, D., Shevliakova, E., and Zhao, M.: The GFDL Global Atmospheric Chemistry-Climate Model AM4.1: Model Description and Simulation Characteristics, J. Adv. Model. Earth Syst., 12, 26, 10.1029/2019ms002032, 2020.

Huang, M., Peng, G. B., Zhang, J. S., and Zhang, S. H.: Application of artificial neural networks to the prediction of dust storms in Northwest China, Glob. Planet. Change, 52, 216-224, 10.1016/j.gloplacha.2006.02.006, 2006.

Hudman, R. C., Moore, N. E., Mebust, A. K., Martin, R. V., Russell, A. R., Valin, L. C., and Cohen, R. C.: Steps towards a mechanistic model of global soil nitric oxide emissions: implementation and space based-constraints, Atmospheric Chemistry and Physics, 12, 7779-7795, 10.5194/acp-12-7779-2012, 2012.

Janssens-Maenhout, G., Crippa, M., Guizzardi, D., Dentener, F., Muntean, M., Pouliot, G., Keating, T., Zhang, Q., Kurokawa, J., and Wankmüller, R.: HTAP_v2.2: a mosaic of regional and global emission grid maps for 2008 and 2010 to study hemispheric transport of air pollution, Atmospheric Chemistry and Physics, 15, 12867-12909, 2015.

Junge, C. E.: GLOBAL OZONE BUDGET AND EXCHANGE BETWEEN STRATOSPHERE AND TROPOSPHERE, Tellus, 14, 363-377, 10.3402/tellusa.v14i4.9563, 1962.

Kim, H. C., Kim, E., Bae, C., Cho, J. H., Kim, B. U., and Kim, S.: Regional contributions to particulate matter concentration in the Seoul metropolitan area, South Korea: seasonal variation and sensitivity to meteorology and emissions inventory, Atmospheric Chemistry and Physics, 17, 10315-10332, 10.5194/acp-17-10315-2017, 2017.

Klimont, Z., Kupiainen, K., Heyes, C., Purohit, P., Cofala, J., Rafaj, P., Borken-Kleefeld, J., and Schopp, W.: Global anthropogenic emissions of particulate matter including black carbon, Atmospheric Chemistry and Physics, 17, 8681-8723, 10.5194/acp-17-8681-2017, 2017.

Kong, L., Tang, X., Zhu, J., Wang, Z. F., Pan, Y. P., Wu, H. J., Wu, L., Wu, Q. Z., He, Y. X., Tian, S. L., Xie, Y. Z., Liu, Z. R., Sui, W. X., Han, L. N., and Carmichael, G.: Improved Inversion of Monthly Ammonia Emissions in China Based on the Chinese Ammonia Monitoring Network and Ensemble Kalman Filter, Environmental Science & Technology, 53, 12529-12538, 10.1021/acsest.9b02701, 2019.

Lee, H. M., Park, R. J., Henze, D. K., Lee, S., Shim, C., Shin, H. J., Moon, K. J., and Woo, J. H.: PM2.5 source attribution for Seoul in May from 2009 to 2013 using GEOS-Chem and its adjoint model, Environmental Pollution, 221, 377-384, 10.1016/j.envpol.2016.11.088, 2017.

Li, J., Wang, Z., Akimoto, H., Yamaji, K., Takigawa, M., Pochanart, P., Liu, Y., Tanimoto, H., and Kanaya, Y.: Near-ground ozone source attributions and outflow in central eastern China during MTX2006, Atmospheric Chemistry and Physics, 8, 7335-7351, 10.5194/acp-8-7335-2008, 2008.

Liu, M. X., Huang, X., Song, Y., Tang, J., Cao, J. J., Zhang, X. Y., Zhang, Q., Wang, S. X., Xu, T. T., Kang, L., Cai, X. H., Zhang, H. S., Yang, F. M., Wang, H. B., Yu, J. Z., Lau, A. K. H., He, L. Y., Huang, X. F., Duan, L., Ding, A. J., Xue, L. K., Gao, J., Liu, B., and Zhu, T.: Ammonia emission control in China would mitigate haze pollution and nitrogen deposition, but worsen acid rain, Proc. Natl. Acad. Sci. U. S. A., 116, 7760-7765, 10.1073/pnas.1814880116, 2019.

Logan, J. A.: An analysis of ozonesonde data for the troposphere: Recommendations for testing 3-D models and development of a gridded climatology for tropospheric ozone, Journal of Geophysical Research-Atmospheres, 104, 16115-16149, 10.1029/1998jd100096, 1999.

Lu, X., Zhang, L., Wu, T. W., Long, M. S., Wang, J., Jacob, D. J., Zhang, F., Zhang, J., Eastham, S. D., Hu, L., Zhu, L., Liu, X., and Wei, M.: Development of the global atmospheric chemistry general circulation model BCC-GEOS-Chem v1.0: model description and evaluation, Geoscientific Model Development, 13, 3817-3838, 10.5194/gmd-13-3817-2020, 2020.

Meijer, E. W., van Velthoven, P. F. J., Thompson, A. M., Pfister, L., Schlager, H., Schulte, P., and Kelder, H.: Model calculations of the impact of NOx from air traffic, lightning, and surface emissions, compared with measurements, Journal of Geophysical Research-Atmospheres, 105, 3833-3850, 10.1029/1999jd901052, 2000.

Monks, P. S., Granier, C., Fuzzi, S., Stohl, A., Williams, M. L., Akimoto, H., Amann, M., Baklanov, A., Baltensperger, U., Bey, I., Blake, N., Blake, R. S., Carslaw, K., Cooper, O. R., Dentener, F., Fowler, D., Fragkou, E., Frost, G. J., Generoso, S., Ginoux, P., Grewe, V., Guenther, A., Hansson, H. C., Henne, S., Hjorth, J., Hofzumahaus, A.,

Huntrieser, H., Isaksen, I. S. A., Jenkin, M. E., Kaiser, J., Kanakidou, M., Klimont, Z., Kulmala, M., Laj, P., Lawrence, M. G., Lee, J. D., Liousse, C., Maione, M., McFiggans, G., Metzger, A., Mieville, A., Moussiopoulos, N., Orlando, J. J., O'Dowd, C. D., Palmer, P. I., Parrish, D. D., Petzold, A., Platt, U., Poschl, U., Prevot, A. S. H., Reeves, C. E., Reimann, S., Rudich, Y., Sellegri, K., Steinbrecher, R., Simpson, D., ten Brink, H., Theloke, J., van der Werf, G. R., Vautard, R., Vestreng, V., Vlachokostas, C., and von Glasow, R.: Atmospheric composition change - global and regional air quality, Atmospheric Environment, 43, 5268-5350, 10.1016/j.atmosenv.2009.08.021, 2009.

Myriokefalitakis, S., Daskalakis, N., Gkouvousis, A., Hilboll, A., van Noije, T., Williams, J. E., Le Sager, P., Huijnen, V., Houweling, S., Bergman, T., Nuss, J. R., Vrekoussis, M., Kanakidou, M., and Krol, M. C.: Description and evaluation of a detailed gas-phase chemistry scheme in the TM5-MP global chemistry transport model (r112), Geoscientific Model Development, 13, 5507-5548, 10.5194/gmd-13-5507-2020, 2020.

Petaja, T., Jarvi, L., Kerminen, V. M., Ding, A. J., Sun, J. N., Nie, W., Kujansuu, J., Virkkula, A., Yang, X. Q., Fu, C. B., Zilitinkevich, S., and Kulmala, M.: Enhanced air pollution via aerosol-boundary layer feedback in China, Sci Rep, 6, 6, 10.1038/srep18998, 2016.

Platnick, S.: MODIS Atmosphere L3 Monthly Product, NASA MODIS Adaptive Processing System, http://dx.doi.org/10.5067/MODIS/MOD08_M3.006, 2015.

Sudo, K., and Akimoto, H.: Global source attribution of tropospheric ozone: Long-range transport from various source regions, Journal of Geophysical Research-Atmospheres, 112, 21, 10.1029/2006jd007992, 2007.

Sun, J. H., Zhao, L. N., Zhao, S. X., and Zhang, R. J.: An integrated dust storm prediction system suitable for East Asia and its simulation results, Glob. Planet. Change, 52, 71-87, 10.1016/j.gloplacha.2006.02.005, 2006.

Tanaka, T. Y., and Chiba, M.: A numerical study of the contributions of dust source regions to the global dust budget, Glob. Planet. Change, 52, 88-104, 10.1016/j.gloplacha.2006.02.002, 2006.

van Geffen, J., Boersma, K. F., Eskesl, H., Sneep, M., ter Linden, M., Zara, M., and Veefkind, J. P.: S5P TROPOMI NO2 slant column retrieval: method, stability, uncertainties and comparisons with OMI, Atmospheric Measurement Techniques, 13, 1315-1335, 10.5194/amt-13-1315-2020, 2020.

Verhoelst, T., Compernolle, S., Pinardi, G., Lambert, J. C., Eskes, H. J., Eichmann, K. U., Fjaeraa, A. M., Granville, J., Niemeijer, S., Cede, A., Tiefengraber, M., Hendrick, F., Pazmino, A., Bais, A., Bazureau, A., Boersma, K. F., Bognar, K., Dehn, A., Donner, S., Elokhov, A., Gebetsberger, M., Goutail, F., de la Mora, M. G., Gruzdev, A., Gratsea, M., Hansen, G. H., Irie, H., Jepsen, N., Kanaya, Y., Karagkiozidis, D., Kivi, R., Kreher, K., Levelt, P. F., Liu, C., Muller, M., Comas, M. N., Piters, A. J. M., Pommereau, J. P., Portafaix, T., Prados-Roman, C., Puentedura, O., Querel, R., Remmers, J., Richter, A., Rimmer, J., Cardenas, C. R., de Miguel, L. S., Sinyakov, V. P., Stremme, W., Strong, K., Van Roozendael, M., Veefkind, J. P., Wagner, T., Wittrock, F., Gonzalez, M. Y., and Zehner, C.: Ground-based validation of the Copernicus Sentinel-5P TROPOMI NO2 measurements with the NDACC ZSL-DOAS, MAX-DOAS and Pandonia global networks, Atmospheric Measurement Techniques, 14, 481-510, 10.5194/amt-14-481-2021, 2021.

Wai, K. M., Wu, S. L., Li, X. L., Jaffe, D. A., and Perry, K. D.: Global Atmospheric Transport and Source-Receptor Relationships for Arsenic, Environmental Science & Technology, 50, 3714-3720, 10.1021/acs.est.5b05549, 2016.

Wang, Z., Uno, I., Yumimoto, K., Pan, X. L., Chen, X. S., Li, J., Wang, Z. F., Shimizu, A., and Sugimoto, N.: Dust Heterogeneous Reactions during Long-Range Transport of a Severe Dust Storm in May 2017 over East Asia, Atmosphere, 10, 17, 10.3390/atmos10110680, 2019.

Wei, Y., Chen, X. S., Chen, H. S., Li, J., Wang, Z. F., Yang, W. Y., Ge, B. Z., Du, H. Y., Hao, J. Q., Wang, W., Li, J. J., Sun, Y. L., and Huang, H. L.: IAP-AACM v1.0: a global to regional evaluation of the atmospheric chemistry model in CAS-ESM, Atmospheric Chemistry and Physics, 19, 8269-8296, 10.5194/acp-19-8269-2019, 2019.

Wiedinmyer, C., Akagi, S. K., Yokelson, R. J., Emmons, L. K., Al-Saadi, J. A., Orlando, J. J., and Soja, A. J.: The Fire INventory from NCAR (FINN): a high resolution global model to estimate the emissions from open burning,

Geoscientific Model Development, 4, 625-641, 10.5194/gmd-4-625-2011, 2011.

Yang, Y., Wang, H., Smith, S. J., Easter, R., Ma, P.-L., Qian, Y., Yu, H., Li, C., and Rasch, P. J.: Global source attribution of sulfate concentration and direct and indirect radiative forcing, Atmospheric Chemistry and Physics, 17, 8903-8922, 10.5194/acp-17-8903-2017, 2017.

Yim, S. H. L., Gu, Y. F., Shapiro, M., and Stephens, B.: Air quality and acid deposition impacts of local emissions and transboundary air pollution in Japan and South Korea, Atmospheric Chemistry and Physics, 19, 13309-13323, 10.5194/acp-19-13309-2019, 2019.

Yin, J., Gao, C. Y., Hong, J., Gao, Z., Li, Y., Li, X., Fan, S., and Zhu, B.: Surface Meteorological Conditions and Boundary Layer Height Variations During an Air Pollution Episode in Nanjing, China, Journal of Geophysical Research-Atmospheres, 124, 3350-3364, 10.1029/2018jd029848, 2019.

Zhang, Q., Zheng, Y. X., Tong, D., Shao, M., Wang, S. X., Zhang, Y. H., Xu, X. D., Wang, J. N., He, H., Liu, W. Q., Ding, Y. H., Lei, Y., Li, J. H., Wang, Z. F., Zhang, X. Y., Wang, Y. S., Cheng, J., Liu, Y., Shi, Q. R., Yan, L., Geng, G. N., Hong, C. P., Li, M., Liu, F., Zheng, B., Cao, J. J., Ding, A. J., Gao, J., Fu, Q. Y., Huo, J. T., Liu, B. X., Liu, Z. R., Yang, F. M., He, K. B., and Hao, J. M.: Drivers of improved PM2.5 air quality in China from 2013 to 2017, Proc. Natl. Acad. Sci. U. S. A., 116, 24463-24469, 10.1073/pnas.1907956116, 2019.

Zhou, F., Ciais, P., Hayashi, K., Galloway, J., Kim, D. G., Yang, C. L., Li, S. Y., Liu, B., Shang, Z. Y., and Gao, S. S.: Re-estimating NH3 Emissions from Chinese Cropland by a New Nonlinear Model, Environmental Science & Technology, 50, 564-572, 10.1021/acs.est.5b03156, 2016.